Reconstruction of Nerve Fiber Orientations in Cell-body Stained Histological Brain Sections using Computational Scattered Light Imaging

auf der Heiden, Franca; Georgiadis, Marios; Zeineh, Michael; Amunts, Katrin; Axer, Markus; Menzel, Miriam

DOI
10.1364/BRAIN.2023.BW1B.3

Publication date
2023

Document Version
Final published version

Published in
Optics and the Brain, BRAIN 2023

Reconstruction of Nerve Fiber Orientations in Cell-body Stained Histological Brain Sections using Computational Scattered Light Imaging

Franca auf der Heiden[1,*], Marios Georgiadis[2], Michael Zeineh[2], Katrin Amunts[1,3], Markus Axer[1], Miriam Menzel[1,4,*]

[1] *Institute of Neuroscience and Medicine (INM-1), Forschungszentrum Jülich GmbH, 52425 Jülich, Germany*
[2] *Department of Radiology, Stanford School of Medicine, Stanford, CA, USA*
[3] *C. and O. Vogt Institute for Brain Research, University Hospital Düsseldorf, 40225 Düsseldorf, Germany*
[4] *Department of Imaging Physics, Delft University of Technology, 2628 CJ Delft, the Netherlands*

[*] *f.auf.der.heiden@fz-juelich.de, m.menzel@fz-juelich.de*

Abstract: We present a method for direct imaging of nerve fiber orientations in cell-body stained histological brain sections, which was not yet possible for paraffin-treated tissue.

1. Introduction

Paraffin embedding for high-quality tissue sectioning is standard in clinical and research histology. In this process, tissue is dehydrated, cleared, and paraffin-embedded. During these steps, a large percentage of lipids is removed, and the layered nanostructure is disturbed; resulting in birefringence loss, so polarization-based techniques (commonly used to visualize nerve fiber directions in post-mortem brain tissue) cannot be used on histology sections. So far, fiber pathways in white matter can only be provided by image processing of specific histology stains but not by direct measurement [1]. Here, we present a novel, birefringence-independent approach to directly measure densely packed nerve fibers in cell-body stained histological brain sections using *Computational Scattered Light Imaging (ComSLI)*. Brain sections are illuminated from different angles with incoherent visible light and the through-scattered light normal to the section plane is detected (Fig. 1A). The modulation of the scattering intensity with the illumination angle reveals the fiber orientations (Fig. 1B) [2]. We show that ComSLI retrieves fiber pathways in paraffin-sectioned human brain sections, stained with Cresyl-violet and silver.

2. Material and Methods

Two human brains (male, 30 and 71 years, no neurological diseases) were formalin-fixed, dehydrated in increasing alcohol series, embedded in paraffin, and coronally cut with a large-scale microtome into 20 µm-thin sections. After deparaffinization, two different stains were applied to highlight neuronal cell bodies: the sections of the first brain were stained with Cresyl-violet (Cv) [3], the sections of the second one with silver (Ag) [4] (Fig. 1C-D, insets in upper left corners). A section from each brain at approximately the same plane was selected and a region containing the corpus callosum (*cc*) and the corona radiata (*cr*) was measured with ComSLI. A diagram of the setup is shown in Fig. 1A: The sample is illuminated from different angles using an LED display ($50\times50\,\mathrm{cm}^2$) with 128×128 individually controllable RGB-LEDs. For each illumination angle, a camera records the through-scattered light normal to the section plane (field of view $1.9\times1.6\,\mathrm{cm}^2$, pixel size 3 µm). The brain sections were measured with angular [5] and scatterometric [2] illumination. For angular illumination, the sections were successively illuminated by a green circle segment with 73 LEDs under an incidence angle of 47° in azimuthal steps of 15° (Cv: exp. time 10 s, gain 10; Ag: exp. time 5 s, gain 5; 4 repetitions for both). The resulting image series was evaluated with the open-source software SLIX [6], which analyzes the position of scattering peaks to compute nerve fiber orientations and visualize them in different colors (Fig. 1C-D). During scatterometric illumination, the sections were successively illuminated by a single white LED at 64×64 different positions (exp. time: 5 s, gain 5). From the resulting image series, scattering patterns (cf. Fig. 1B) were computed for each image pixel.

3. Results and Discussion

The corpus callosum (*cc*) is a nerve fiber bundle with mostly parallel, in-plane fibers in the coronal section plane. Fig. 1C-D show the color-coded fiber orientation maps obtained by ComSLI. The zoom-ins in Fig. 1E-F display the corresponding fiber orientation vectors. The fibers in the *cc* run mostly diagonally (green/yellow) with some distinct bundles oriented horizontally (red). The oval shape of the scattering patterns (exemplary shown in Fig. 1B, marked with * in Fig. 1F) agrees with the expected fiber orientation. For reference, Fig.1G shows a color-coded

comparable human brain area measured with Polarized Light Imaging [7]. Overall, the signal from the silver stained section is stronger than from the Cresyl-violet stained section; resulting in more colored pixels in Fig. 1D. ComSLI yields promising results especially for mostly parallel, in-plane fibers in the *cc*. Even though the birefringent properties had been lost during sample preparation, fiber directions that match the expected fiber anatomy in the *cc* were successfully obtained both for Cresyl-violet and silver stained brain sections. Regions with crossing fibers seem to have a lower signal to noise ratio, but optimizing measurement parameters (e.g. brighter illumination, longer exposure) might solve this issue. The influence of different stains still needs to be studied.
This study remains a proof-of-principle and therefore, the full information contained in the scattering patterns has not yet been analyzed in depth. ComSLI seems to be a promising imaging technique to directly measure the nerve fiber architecture of paraffin-treated, stained brain tissue, using low-cost, standard optical components and existing histological sections. This opens up the possibility to combine histological insights from cell body distributions with detailed mapping of nerve fiber architecture in the brain.

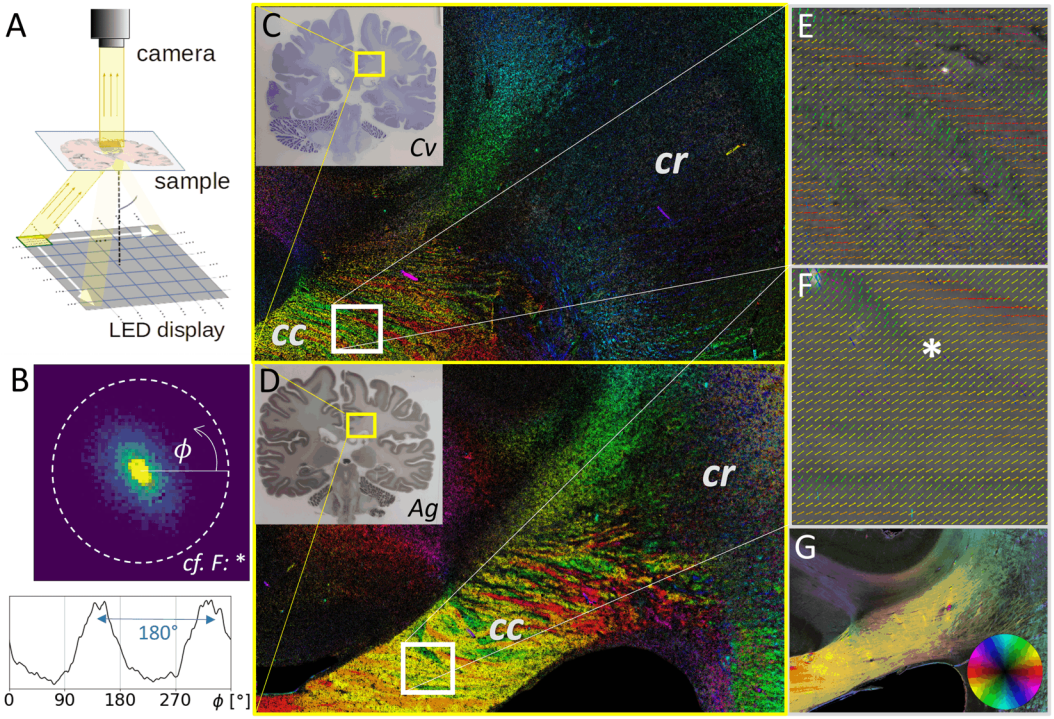

Fig. 1. (**A**) ComSLI setup. (**B**) Exemplary scattering pattern and intensity profile, taken from * in (F). (**C, D**) ComSLI results of a coronal human brain section stained with Cresyl-violet (Cv) and with silver (Ag). The insets in the upper left corners show a photograph of the entire brain sections. The color-coded fiber orientation maps for each image pixel are shown for the measured region (yellow rectangles) according to the color wheel (*cc*: corpus callosum, *cr*: corona radiata). (**E, F**) Fiber orientations visualized as colored lines, overlaid for 15 x 15 image pixels, shown exemplary for a *cc* region (white rectangles). (**G**) Comparable *cc* region measured with Polarized Light Imaging [7].

References

1. R. Schurr and A. Mezer, “The glial framework reveals white matter fiber architecture in human and primate brains,” *Science*, vol. 374, no. 6568, pp. 762–767, 2021.
2. M. Menzel *et al.*, “Scatterometry Measurements with Scattered Light Imaging Enable New Insights into the Brain’s Nerve Fiber Architecture,” *Front. Neuroanat.*, 08 2021.
3. E. Aescht *et al.*, “Färbungen,” in *Romeis Mikroskopische Technik*, pp. 181–297, Heidelberg: SAV, 2010.
4. H. Uylings, K. Zilles, and G. Rajkowska, “Optimal staining methods for delineation of cortical areas and neuron counts in human brains,” *NeuroImage*, vol. 9, no. 4, pp. 439–445, 1999.
5. M. Menzel *et al.*, “Scattered Light Imaging: Resolving the substructure of nerve fiber crossings in whole brain sections with micrometer resolution,” *NeuroImage*, vol. 233, p. 117952, 2021.
6. J. Reuter and M. Menzel, “SLIX: A Python package for fully automated evaluation of Scattered Light Imaging measurements on brain tissue,” *J. Open Source Softw.*, vol. 5, no. 54, p. 2675, 2020.
7. M. Axer and K. Amunts, “Scale matters: The nested human connectome,” *Science*, vol. 378, no. 6619, pp. 500–504, 2022.